NIH Public Access
Author Manuscript
Hepatology. Author manuscript; available in PMC 2008 January 10.

Published in final edited form as:
Hepatology. 2007 November ; 46(5): 1464–1475.

Sinusoidal Endothelial Cell Repopulation Following Ischemia/Reperfusion Injury in Rat Liver Transplantation

Donna Beer Stolz[1,2], **Mark A. Ross**[1], **Atsushi Ikeda**[3,4], **Koji Tomiyama**[3,4], **Takashi Kaizu**[3,4], **David A. Geller**[3,4], and **Noriko Murase**[3,4]

1 *Cell Biology and Physiology and the Center for Biologic Imaging, University of Pittsburgh, Pittsburgh, PA*

2 *Center for Vascular Remodeling and Regeneration, University of Pittsburgh, Pittsburgh, PA*

3 *Thomas E. Starzl Transplantation Institute, University of Pittsburgh, Pittsburgh, PA*

4 *Department of Surgery, University of Pittsburgh, Pittsburgh, PA*

Abstract

We evaluated the kinetics by which rat liver sinusoidal endothelial cells (LSECs) are repopulated in the reperfused transplanted liver after 18 hours of cold ischemic storage. We found that the majority of LSECs in livers cold-stored for 18 hours in University of Wisconsin solution are seriously compromised and often are retracted before transplantation. Sinusoids rapidly re-endothelialize within 48 hours of transplantation, and repopulation is coincident with up-regulation of hepatocyte vascular endothelial growth factor expression and vascular endothelial growth factor receptor-2 expression on large vessel endothelial cells and repopulating LSECs. Although re-endothelialization occurs rapidly, we show here, using several high-resolution imaging techniques and 2 different rat liver transplantation models, that engraftment of bone marrow–derived cells into functioning LSECs is routinely between 1% and 5%.

Conclusion—Bone marrow plays a measurable but surprisingly limited role in the rapid repopulation and functional engraftment of bone marrow–derived LSECs after cold ischemia and warm reperfusion.

Liver transplantation is the therapy of choice for patients with end-stage liver disease. However, the surgical procedures involved in transplantation require cold preservation and warm reperfusion of grafts, resulting in varying degrees of ischemia/reperfusion (I/R) injury in all liver grafts. I/R injury remains a major problem complicating posttransplantation patient care and subsequent recovery. Determining the mechanisms responsible for I/R injury associated with liver transplantation may lead to strategies to reduce organ damage. This could have enormous impact on patient care in the early posttransplantation period and improve long-term outcome.

I/R injury is a progression of events involving many interconnected factors that have been intricately documented in the last decade,[1–9] including detrimental effects of Kupffer cell activation, cholestasis, hepatocellular ballooning, neutrophil infiltration, and apoptosis/necrosis of both liver sinusoidal endothelial cells (LSECs) and hepatocytes.[6,8,9] It is also well known that LSECs are particularly vulnerable to transplant-induced I/R injury.[10–12] Morphological studies have characterized LSEC alteration during cold storage as retraction and detachment of cell bodies. Subsequent warm reperfusion augments injury, progressing to nearly complete denudation of the LSEC lining.[3,10–12] However, there is a paucity of data

Address reprint requests to: Donna Beer Stolz, Ph.D., Cell Biology and Physiology, BST South 221, University of Pittsburgh Medical School, Pittsburgh, PA 15261. E-mail: dstolz@pitt.edu; fax: 412-648-2797.

Potential conflict of interest: Nothing to report.

NIH-PA Author Manuscript
NIH-PA Author Manuscript
NIH-PA Author Manuscript

NIH-PA Author Manuscript

NIH-PA Author Manuscript

NIH-PA Author Manuscript

regarding the nature of LSEC recovery and regeneration following injury. We herein detail the LSEC response after cold storage and early postperfusion periods. Particular attention is paid to LSEC ultrastructure and the involvement of bone marrow– derived (BM) cells during LSEC repopulation.

Materials and Methods

Animals

Animals were treated according to institutional animal care and use committee guidelines and maintained in a laminar-flow, pathogen-free atmosphere. Male Lewis (LEW, $RT1^l$) and Brown Norway (BN, $RT1^n$) rats (200–300 g) were obtained from Harlan Sprague-Dawley, Inc. (Indianapolis, IN). Enhanced green fluorescent protein (EGFP)-transgenic and wild-type (WT) Sprague-Dawley rats[13] were obtained from Japan SLC Inc. (Hamamatsu, Japan). EGFP expression is under the control of the cytomegalovirus enhancer and the chicken β-actin promoter derived from the expression vector, pCAGGS. We maintain a breeding colony of EGFP transgenics, inbreeding the Sprague-Dawley background for >12 generations, confirming via skin grafting that this colony is syngeneic. Liver transplantation between EGFP heterozygotes and WT animals are considered syngeneic.

Reagents

Reagents were purchased from Sigma Chemical Company (St. Louis, MO) unless noted otherwise.

Orthotopic Liver Transplantation

Liver harvesting and orthotopic liver transplantation (OLTx) without hepatic arterial reconstruction were described.[14] After harvest, grafts were kept in University of Wisconsin solution at 4°C for 18 hours of cold ischemic time (CIT) and orthotopically transplanted into designated recipients. Eighteen-hour CIT induced significant cold I/R injury in liver grafts without mortality.[15,16] Hepatic injury was assessed via serum alanine transaminase levels, which at 24 hours increased to a peak of 4209 ± 1551 U/L from the normal value of 56.0 ± 9.8 U/L. Recipient animals were sacrificed at the indicated times, and liver graft samples were obtained for specific evaluation as described below.

Immunofluorescence Microscopy

Livers were perfusion-fixed with 2% paraformaldehyde in phosphate-buffered saline (PBS) after PBS clearance through the portal vein. Fixed tissues were immersed in 2.3 M sucrose in PBS overnight at 4°C, then frozen in liquid nitrogen– cooled isopentane and stored at −80°C until sectioned. Livers were sectioned at 6 μm, and immunostaining was performed as described[17] using the antibodies and reagents listed in Table 1. LSECs fixed on coverslips were perme-abilized with 0.1% Triton X-100 before staining. Samples were coverslipped using gelvatol[17] and viewed on a Fluo-view 1000 confocal microscope (Olympus, Center Valley, PA). Propidium iodide (PI) infusion and in situ staining were performed on liver grafts as described[18] prior to staining for SE-1.

Electron Microscopy

Scanning electron microscopy (SEM) and transmission electron microscopy (TEM) were performed on 2.5% glutaraldehyde in PBS perfusion-fixed liver and LSECs on coverslips as described.[19] Immuno-SEM was performed on 2% paraformaldehyde perfusion-fixed liver as for immunofluorescence, but tissue was not incubated in sucrose and frozen. Surface labeling was performed essentially as described[20] on 2–3-mm-thick liver slices. After labeling, tissue was dehydrated through graded ethanol (30%–100%), critical point dried (Emscope, CPD 750,

NIH-PA Author Manuscript

NIH-PA Author Manuscript

NIH-PA Author Manuscript

Ashford, Kent, UK), and overcoated with carbon (108Carbon/A Coater, Watford, UK). Tissues were visualized on a JEM-6335F scanning electron microscope (JEOL, Peabody, MA). Backscattered and secondary electron images were taken in tandem to detect gold labeling on the cell surfaces coincident with cellular morphology.

Sinusoidal Cell Isolation

To characterize the origin of the cells repopulating liver sinusoids, we magnetically tagged cells in contact with the blood to facilitate subsequent isolation. Labeled cells are preferentially removed from the postparenchymal pellet using standard magnetic bead columns and evaluated for specific cell markers. This technique is a modification of the cationic colloidal silica perfusion technique[21] coupled with the 2-stage collage-nase perfusion protocol.[22] Solutions were maintained at 37°C and perfused at 12 mL/minute. Cells were prepared for isolation by clearing blood with MES-buffered saline (20 mM 2-[N-Morpholino]ethanesulfonic acid, 150 mmol/L NaCl; pH 5.0) followed by 50 mL of 50-nm colloidal magnetite (fluidMAG-PEI, Chemicell, Berlin, Germany) diluted 1:500 with MES-buffered saline. Livers were digested via perfusion with 250 mL collagenase solution (0.168 mg/mL type IV collagenase, 11 mM $CaCl_2$ in MES-buffered saline). Liver was harvested and cells were dispersed through 100-μm mesh nylon. Hepatocytes were pelleted from the cell suspension at 50*g* for 10 minutes, while remaining nonparenchymal cells (NPCs) were pelleted from the supernatant at 350*g* for 10 minutes. Hepatocytes were washed and repelleted 3 times, retaining and pooling supernatants. The pooled supernatants were centrifuged at 350*g*, and magnetized cells were isolated via magnetic separation using Miltenyi MACS LS columns (Miltenyi Biotec, Auburn, CA). In rats weighing 200–250 g, the magnetite perfusion routinely yields 5–10 × 10^7 liver endothelial cells, which is greater than the amount obtained with other common isolation techniques[23,24] and comparable to centrifugal elutriation protocols.[20] Additionally, this technique isolates all cells from the sinusoid. These cells can then be used for other experiments. For culture, LSECs were re-suspended in complete growth medium (EBM2 basal medium plus EGM2 Bulletkit; Cambrex, Walkersville, MD) and plated directly onto 50 μg/mL collagen I absorbed onto 12-mm coverslips.

Flow Cytometry (Fluorescence-Activated Cell Sorting)

Sinusoidal NPCs isolated after OLTx were analyzed by staining for SE-1, CD31, ED2 (CD163), and OX1 (CD45) coincident with endogenous EGFP expression (Table 1, Table 2). Cells were fixed in 2% paraformaldehyde in PBS and analyzed using a Coulter Elite ESP (Coulter Corp., Miami, FL). Isotype-matched nonspecific antibodies were used as controls. Cell suspensions examined via fluorescence-activated cell sorting (FACS) were retained and spun onto slides (Shandon Cytospin 2, Thermo Electron, Waltham, MA), labeled with nuclear stain (Hoechst), and examined via confocal microscopy.

Statistical Analysis

Data are represented as the mean ± standard deviation. Comparisons between groups at different time points were performed via Student *t* test or analysis of variance using Statview (Abacus Concepts, Inc., Berkeley, CA). A *P* value of less than 0.05 was considered significant.

Results

In initial studies, we evaluated the response of LSECs to 18-hour CIT and subsequent transplantation with relationship to vascular endothelial growth factor (VEGF) and vascular endothelial growth factor receptor-2 (VEGF-R2) expression. Following syngeneic OLTx of 18-hour CIT LEW rat livers, we observed increased hepatic VEGF expression 12–48 hours post-OLTx (Fig. 1A). Coincident with hepatic VEGF expression, increased VEGF-R2 expression was observed on large vessel endothelial cells and LSECs (Fig. 1B). Most striking,

NIH-PA Author Manuscript

NIH-PA Author Manuscript

NIH-PA Author Manuscript

however, was the loss of the specific rat LSEC marker, SE-1,[24,25] from the liver within 1 hour after OLTx (Fig. 1B). Although normal rat liver had an abundant SE-1 signal showing typical vascular distribution throughout the liver, after 1 hour of reperfusion, the SE-1 signal was significantly reduced throughout the lobule. However, SE-1 expression was restored rapidly after OLTx; the SE-1 signal increased slightly by 6 hours and completely recovered by 24–48 hours (Fig. 1B). These results suggest prompt recovery/regeneration of LSECs 24–48 hours after hepatic I/R injury is tightly associated with hepatocyte VEGF expression.

To determine if the decline of the SE-1 signal was the direct result of LSEC loss, and not reduction of the SE-1 protein in LSECs, we undertook a series of ultrastructural analyses paralleling the immunofluorescence timepoints after OLTx. As shown previously,[4] 18-hour CIT in University of Wisconsin solution induced significant LSEC I/R injury, and additional damage resulted from subsequent warm reperfusion.[11] SEM was conducted to investigate LSEC ultrastructural changes during the restorative period after OLTx. Normal liver showed intact LSECs with contiguous cells and fenestrations arranged in sieve plates (Fig. 2; control). In contrast, grafts at the end of 18-hour CIT showed significant damage with large areas of denuded sinusoidal lining and retracted cells (Fig. 2; 18Hr CIT). At 1 hour post-OLTx, the sinusoid remained denudated (Fig. 2; 1Hr Tx), and at 3–6 hours, leukocytes were adherent to the sinusoidal surface, with some evidence for LSEC restoration (Fig. 2; 3Hr Tx, 6Hr Tx). By 24 hours, the sinusoid lining was nearly restored, but the porosity was greatly reduced compared with control livers (Fig. 2, 24Hr Tx). This reduction in porosity has been observed in regenerating LSECs after partial hepatectomy.[19] This approach proves the value of ultrastructural analysis, because routine histopathology detects minimum pathological LSEC changes in preserved liver grafts.[26]

Additional analysis using TEM showed similar morphological changes, but with greater intracellular detail (Fig. 3). After 18-hour CIT, many LSECs appeared necrotic but maintained attachment to the space of Disse. As early as 1 hour post-OLTx and continuing through 6 hours post-OLTx, the sinusoidal surface appeared denuded, but deposition of platelets, lymphocytes, and macrophages (filled with cellular debris) were observed within the sinusoids. By 24 hours, most of the sinusoidal surface was reconstituted, although the majority of macrophages showed many inclusion bodies, indicating recent active phagocytosis of cellular debris.

We then evaluated LSEC viability in situ with PI.[18] PI intercalates into nonviable cell nuclear DNA, gaining nuclear access via disrupted membranes. As shown in Fig. 4, control liver showed no PI uptake in any cells. After 18-hour CIT, many SE-1^+ cells displayed PI uptake indicating LSEC death, and a substantial increase in LSEC death was observed 1 hour post-OLTx. As expected, at early times after OLTx, hepatocytes were refractory to PI uptake.

Because 18-hour CIT induces significant LSEC damage with many retracted cells, we were interested in determining if these compromised LSECs could detach from the sinusoid upon reperfusion. To characterize detached cells from CIT liver grafts, we collected cells flushed out of control, 18-hour, and 48-hour cold-stored livers. When grafts were perfused with PBS at the end of 18-hour cold University of Wisconsin solution preservation, $0.3–3.8 \times 10^5$ cells per gram liver weight were released into effluents (Table 3) with the total numbers of cells in the wash $0.56–3.96 \times 10^6$. These numbers from the 18-hour preserved grafts were not significantly different from normal livers, suggesting that the number of cells released into effluent washes from preserved grafts was small. FACS analysis of released cells demonstrated that approximately 40%–50% of cells were $CD45^+$ leukocytes, including $ED2^+$ (CD163) Kupffer cells; SE-1^+ cells released into effluents accounted for approximately 50% of the total cells. Minimum annexin V expression was observed on LSECs at any time, suggesting that released cells were not apoptotic. TEM analysis had previously indicated that LSEC death at this time proceeds via the necrotic pathway (Fig. 2; 18Hr CIT).

NIH-PA Author Manuscript

NIH-PA Author Manuscript

NIH-PA Author Manuscript

I/R injury resulted in significant LSEC denudation soon after warm reperfusion; however, LSECs rapidly recover by 24–48 hours after OLTx. Due to this rapid recovery, LSEC repopulation could be explained as replacement from recipient endothelial progenitor cells (local or BM-derived). Alternatively, the prompt recovery may suggest that some LSECs are retracted, but not completely denudated, and quickly divide to reform sinusoidal lining. To determine the origin of repopulated LSECs at 3 days after transplantation, 2 sets of transplantation experiments were performed. In fully allogeneic BN to LEW rat strain combination, the phenotypes of LSECs were analyzed using monoclonal antibodies specific for donor and recipient major histocompatibility complex (MHC) antigens.[27] Additionally, WT graft to EGFP recipient liver transplantation was performed, and the presence and engraftment of recipient $EGFP^+$ -BM tagged cells was evaluated in the WT graft.

Initial experiments were performed in the allogeneic OLTx model using BN donor livers transplanted into LEW rat recipients after 18-hour CIT University of Wisconsin solution storage. Three days after OLTx, livers were perfusion-fixed as described in Materials and Methods and processed for immunofluorescence and immuno-SEM using a monoclonal antibody (L21-6) to the LEW MHC class II antigen to identify cells of recipient origin in the graft sinusoids.[27] Perfusion clearance, followed by fixation, ensured that cells observed in the tissue were resident and adherent and not simply passing through the liver at the time of sacrifice. BN livers showed minimal infiltration of recipient LEW cells, and these cells did not display the characteristic flattened LSEC shape (Fig. 5A). Monoclonal antibody (OX27) for donor BN MHC class I antigens was observed throughout the donor liver, as expected (Fig. 5B).

We expanded the study to evaluate the ultrastructural colocalization of the LEW-MHC class II antigen within the fenestrated endothelium—the functional and morphological hallmark of LSECs— using immuno-SEM. Infrequently (1 cell in several hundred examined), fenestrated endothelium did show positive surface backscatter signal from the L21-6 antibody, indicating that that particular LSEC was BM-derived (Fig. 5C–D). Given the scarcity of these dual positive cells, it was difficult to quantify the actual BM engraftment into LSECs using this technique. Most $L21\text{-}6^+$ cells had a rounded appearance and were adherent to vessel surfaces (Fig. 5D–E), indicating they were likely leukocytes. To this end, we modified our approach and used the EGFP transgenic rat model to further characterize this observation.

After OLTx of 18-hour CIT WT liver into $EGFP^+$ syngeneic recipients, the timing of LSEC denudation and repopulation proceeded as for the LEW syngeneic or BN to LEW allogeneic OLTx, with restitution of the sinusoidal lining by $SE\text{-}1^+$ cells complete by 48 hours after OLTx (data not shown). WT livers showed significant infiltration of $EGFP^+$ recipient cells at all times after OLTx, from 1 hour to 36 days posttransplantation. At the extended time points, such as 3–36 days post-OLTx, stringent conditions were set up to identify LSECs that may be recipient BM-derived $EGFP^+$ cells; this required continuous plasma membrane staining by SE-1, in addition to showing a flattened nucleus within the perimeter of EGFP and SE-1 staining. Figure 6A shows a typical confocal field in such a liver. Although there are many $EGFP^+$ cells, very few met the criteria identifying them as BM-derived LSECs, as highlighted in Fig. 6B–D. Interestingly, we rarely observed $EGFP^+$ hepatocytes in the hundreds of sections that were evaluated (Fig. 6A–B), but these were not enumerated for this study. Counting cells using confocal microscopy in tissue sections yielded $3.12 \pm 1.65\%$ dual $EGFP^+/SE\text{-}1^+$ cells, counting at least 1500 $SE\text{-}1^+$ cells from multiple sections and livers. This percentage did not vary significantly with increased time after OLTx. The majority of the $EFGP^+$ cells were not $SE\text{-}1^+$, so we assessed costaining with CD45, ED1 (CD68), and ED2 (CD163), to identify other NPCs. A very high percentage of $EGFP^+$ cells were $CD45^+$ in the sections (Fig. 6E); interestingly, though, very few $EGFP^+$ cells were positive for the macrophage/monocyte marker CD68 (Fig. 6F).

NIH-PA Author Manuscript

NIH-PA Author Manuscript

NIH-PA Author Manuscript

To better identify and quantify sinusoidal cells that were also $EGFP^+$ and therefore BM-derived, we developed a nonimmunological technique to isolate cells within the sinusoidal space that are in contact with the blood (Fig. 7A). Perfusion of the liver vasculature with 50-nm cationic magnetite adheres to all exposed surfaces (Fig. 7B). These magnetically tagged sinusoidal NPCs were preferentially removed from the total NPC population by magnetic column. These cells could be cultured and displayed the attributes of LSECs in vitro, including maintenance of fenestrations and SE-1 signal with concurrent uptake of Di-I-acetylated-LDL. (Fig 7C–F).

Freshly isolated, magnetized cells were subjected to FACS analysis with similar results to those observed by counting directly in the tissue (Fig. 8A). $EGFP^+$ costained with $SE\text{-}1^+$ or $CD31^+$ cells represented 1% and 0.5% (2.2% and 1.0% of total $SE\text{-}1^+$ or $CD31^+$), respectively. $EGFP^+/CD45^+$ cells accounted for 38.2% of the BM-derived cells in the transplanted liver. Immunofluorescence imaging of the cytospins of these FACS analyzed cells showed similar ratios (Fig. 8B). Table 3 quantifies the NPC cell-specific markers that colocalized with the EGFP of BM-derived cells. Although the general endothelial population ($SE1^+/CD31^+$) and leukocytes ($CD45^+$) accounted for the majority of the NPCs magnetically isolated from the sinusoid, 41% of the $CD45^+$ cells were also $EGFP^+$, while only approximately 4% of $SE\text{-}1^+$ were $EGFP^+$.

Discussion

There is great interest surrounding the clinical significance of recipient BM-derived cells engrafting into donor organs and transdifferentiating into various cell types within the tissue. The seminal work of Isner and colleagues first brought attention to the phenomenon that circulating endothelial progenitors could be recruited to and engraft into sites of active angiogenesis.[28] Given the systemic nature of the vasculature and its continuous interactions with the BM-stem cell compartment, BM-endothelial, precursor-driven, postfetal vasculogenesis has been reputed to occur with great frequency,[29] whereas others report that actual engraftment events are rare.[30,31] However, the majority of reports confirm events wherein exogenously delivered endothelial cell precursors “contribute” to neovessel growth and vascularity but provide no direct quantitative evidence for functional engraftment.[32] Nonetheless, apparent discrepancies are expected, because each neovascular growth condition may provide unique microenvironmental signals to drive BM-derived cell engraftment.[31,32] These cues and conditions remain poorly understood.

The LSEC repopulation paradigm after OLTx I/R injury represents a reasonable system to evaluate such events given the severity of LSEC damage and the rapidity of their renewal. Previous studies in human transplanted liver biopsies report a wide range of BM-derived cells differentiating into liver endothelium (Table 4). All these studies have taken advantage of the Y chromosome signal in sex-mismatched female-into-male OLTx for documenting BM derivation of transdifferentiation events. In humans, methods for following such events are hindered by the BM markers that can be ethically used. It is also recognized that studies relying on one method of characterization are often subject to misinterpretation with regard to engraftment numbers.[31] The choice of LSEC marker can also be brought into question, because many are secreted proteins (vWF, factor VIII) that may be deposited on sinusoidal surfaces, especially during liver pathologies such as I/R injury or whose expression may change as a result of culture conditions.[33] Additionally, the typical pan-endothelial marker CD31 is not highly expressed in LSECs in situ.[20,33]

With these limitations in human studies, we sought to characterize LSEC repopulation using the well-described rat I/R OLTx model, because BN-LEW allogeneic and EGFP syngeneic strains possess sensitive markers to identify host BM-derived cells in these transplant systems.

NIH-PA Author Manuscript

NIH-PA Author Manuscript

NIH-PA Author Manuscript

Additionally, the antigen SE-1, an LSEC-specific surface marker, is critical to evaluating the origin and differentiation state of the LSECs using FACS and confocal imaging[24,25] and is a more reliable marker than CD31[20,33] for LSECs in this setting.

Consistent with previous reports, we confirmed that LSECs are severely injured in the early time points after OLTx.[10–12] In this study, we show that injury is measurable and significantly increased immediately after cold ischemic storage before OLTx. Subsequently, we observed rapid repopulation of LSECs after I/R injury closely paralleled hepatic VEGF expression, coincident with VEGF-R2 up-regulation on both large vessel endothelial cells and LSECs. Although VEGF has been shown to be induced following I/R injury,[34] here we show that coinduction of VEGF-R2 on endothelium indicates these events are tightly coordinated. VEGF/VEGF-R interactions are known contribute to endothelial precursor-driven neovascularization.[35] This observation, coupled with the rapid loss and repopulation of LSECs after OLTx, prompted our evaluation of the potential recruitment and engraftment of BM-derived endothelial precursors to revascularization sites. The two transplantation systems we used showed similar results, with BM-derived cells contributing to LSEC repopulation between 1% and 5%. Also, the pattern of repopulation of the BM-derived LSECs indicates that these are sporadic events and not the result of clonagenic expansion of an early single-cell engraftment.

The discrepancies between our results and some listed in Table 4 could be attributed to differential response in the species used.[36–39] Portal and central vein endothelial repopulation of male BM-derived cells in female human and mouse liver reported by Gao et al.[36] were never observed in our rat systems up to 36 days post-OLTx. We did see substantial $EGFP^+$ cells just under the endothelium in the large vessel zones (Fig. 6A). However, it is more likely that the sensitivity and specificity of the Y chromosome assays used to identify BM-derivation are prone to artifact, and additional BM and cell-specific markers are required to positively identify these as colocalizing signals. Regardless, it is clear that BM-derived cells do engraft into functional LSECs. Further experimentation will be required to determine if such a limited engraftment is clinically relevant in the context of I/R liver transplantation.

Acknowledgements

The authors acknowledge the generosity of Dr. Katsuhiko Enomoto, Akita University, Japan, for generously supplying the SE-1 antibody and Dr. Masaru Okabe, Osaka University, Japan, for the EGFP rats. We thank Mara Sullivan, Ana Lopez, Anna Romanosky, and Amy Breucken for superb technical assistance and Dr. Hideyoshi Toyokawa for maintenance of the EFGP rat colony.

Supported by National Institutes of Health grants R01CA76541 (to D.B.S.), R01 DK54232 and R01 DK071753 (to N.M.), and R01 DK062313 (to D.A.G.).

References

1. Clavien PA, Harvey PR, Strasberg SM. Preservation and reperfusion injuries in liver allografts. An overview and synthesis of current studies. Transplantation 1992;53:957–978. [PubMed: 1585489]
2. Jaeschke H. Preservation injury: mechanisms, prevention and consequences. J Hepatol 1996;25:774–780. [PubMed: 8938560]
3. McKeown CM, Edwards V, Phillips MJ, Harvey PR, Petrunka CN, Strasberg SM. Sinusoidal lining cell damage: the critical injury in cold preservation of liver allografts in the rat. Transplantation 1988;46:178–191. [PubMed: 3043774]
4. Caldwell-Kenkel JC, Currin RT, Tanaka Y, Thurman RG, Lemasters JJ. Reperfusion injury to endothelial cells following cold ischemic storage of rat livers. Hepatology 1989;10:292–299. [PubMed: 2668147]
5. Lemasters JJ, Bunzendahl H, Thurman RG. Reperfusion injury to donor livers stored for transplantation. Liver Transpl Surg 1995;1:124–138. [PubMed: 9346554]

NIH-PA Author Manuscript

NIH-PA Author Manuscript

NIH-PA Author Manuscript

6. Ikeda T, Yanaga K, Kishikawa K, Kakizoe S, Shimada M, Sugimachi K. Ischemic injury in liver transplantation: difference in injury sites between warm and cold ischemia in rats. Hepatology 1992;16:454–461. [PubMed: 1639355]
7. Fondevila C, Busuttil RW, Kupiec-Weglinski JW. Hepatic ischemia/reperfusion injury—a fresh look. Exp Mol Pathol 2003;74:86–93. [PubMed: 12710939]
8. Casillas-Ramirez A, Mosbah IB, Ramalho F, Rosello-Catafau J, Peralta C. Past and future approaches to ischemia-reperfusion lesion associated with liver transplantation. Life Sci 2006;79:1881–1894. [PubMed: 16828807]
9. Miyagawa Y, Imamura H, Soeda J, Matsunaga K, Mochida S, Fujiwara K, et al. Fate of hepatocyte and sinusoidal lining cell function and kinetics after extended cold preservation and transplantation of the rat liver. Liver Transpl 2002;8:370–381. [PubMed: 11965582]
10. Myagkaya GL, van Veen HA, James J. Ultrastructural changes in the rat liver during Euro-Collins storage, compared with hypothermic in vitro ischemia. Virchows Arch B Cell Pathol Incl Mol Pathol 1987;53:176–182. [PubMed: 2888236]
11. Caldwell-Kenkel JC, Currin RT, Tanaka Y, Thurman RG, Lemasters JJ. Kupffer cell activation and endothelial cell damage after storage of rat livers: effects of reperfusion. Hepatology 1991;13:83–95. [PubMed: 1988348]
12. Clavien PA. Sinusoidal endothelial cell injury during hepatic preservation and reperfusion. Hepatology 1998;28:281–285. [PubMed: 9695988]
13. Ito T, Suzuki A, Imai E, Okabe M, Hori M. Bone marrow is a reservoir of repopulating mesangial cells during glomerular remodeling. J Am Soc Nephrol 2001;12:2625–2635. [PubMed: 11729231]
14. Kamada N, Calne RY. A surgical experience with five hundred thirty liver transplants in the rat. Surgery 1983;93:64–69. [PubMed: 6336859]
15. Takahashi Y, Ganster RW, Gambotto A, Shao L, Kaizu T, Wu T, et al. Role of NF-kappaB on liver cold ischemia-reperfusion injury. Am J Physiol Gastrointest Liver Physiol 2002;283:G1175–G1184. [PubMed: 12381532]
16. Kaizu T, Ikeda A, Nakao A, Takahashi Y, Tsung A, Kohmoto J, et al. Donor graft adenoviral iNOS gene transfer ameliorates rat liver transplant preservation injury and improves survival. Hepatology 2006;43:464–473. [PubMed: 16496305]
17. Ross MA, Sander CM, Kleeb TB, Watkins SC, Stolz DB. Spatiotemporal expression of angiogenesis growth factor receptors during the revascularization of regenerating rat liver. Hepatology 2001;34:1135–1148. [PubMed: 11732003]
18. Tsuchihashi S, Tamaki T, Tanaka M, Kawamura A, Kaizu T, Ikeda A, et al. Pyrrolidine dithiocarbamate provides protection against hypothermic preservation and transplantation injury in the rat liver: the role of heme oxygenase-1. Surgery 2003;133:556–567. [PubMed: 12773984]
19. Wack KE, Ross MA, Zegarra V, Sysko LR, Watkins SC, Stolz DB. Sinusoidal ultrastructure evaluated during the revascularization of regenerating rat liver. Hepatology 2001;33:363–378. [PubMed: 11172338]
20. DeLeve LD, Wang X, Hu L, McCuskey MK, McCuskey RS. Rat liver sinusoidal endothelial cell phenotype is maintained by paracrine and autocrine regulation. Am J Physiol Gastrointest Liver Physiol 2004;287:G757–G763. [PubMed: 15191879]
21. Stolz DB, Ross MA, Salem HM, Mars WM, Michalopoulos GK, Enomoto K. Cationic colloidal silica membrane perturbation as a means of examining changes at the sinusoidal surface during liver regeneration. Am J Pathol 1999;155:1487–1498. [PubMed: 10550305]
22. Seglen O. Preparation of isolated rat liver cells. Methods Cell Biol 1976;13:29–83. [PubMed: 177845]
23. Braet F, De Zanger R, Sasaoki T, Baekeland M, Janssens P, Smedsrod B, et al. Assessment of a method of isolation, purification, and cultivation of rat liver sinusoidal endothelial cells. Lab Invest 1994;70:944–952. [PubMed: 8015298]
24. Tokairin T, Nishikawa Y, Doi Y, Watanabe H, Yoshioka T, Su M, et al. A highly specific isolation of rat sinusoidal endothelial cells by the immunomagnetic bead method using SE-1 monoclonal antibody. J Hepatol 2002;36:725–733. [PubMed: 12044521]
25. Ohmura T, Enomoto K, Satoh H, Sawada N, Mori M. Establishment of a novel monoclonal antibody, SE-1, which specifically reacts with rat hepatic sinusoidal endothelial cells. J Histochem Cytochem 1993;41:1253–1257. [PubMed: 8331290]

NIH-PA Author Manuscript

NIH-PA Author Manuscript

NIH-PA Author Manuscript

26. Kakizoe S, Yanaga K, Starzl TE, Demetris AJ. Evaluation of protocol before transplantation and after reperfusion biopsies from human orthotopic liver allografts: considerations of preservation and early immunological injury. Hepatology 1990;11:932–941. [PubMed: 2365291]
27. Yagihashi A, Takahashi S, Murase N, Starzl TE, Iwaki Y. A monoclonal antibody (L21-6) recognizing an invariant chain expressed on the cell surface in rats with the exception of the BN (RT1n): a study of tissue and strain distributions. Transplant Proc 1995;27:1519–1521. [PubMed: 7725397]
28. Asahara T, Murohara T, Sullivan A, Silver M, van der Zee R, Li T, et al. Isolation of putative progenitor endothelial cells for angiogenesis. Science 1997;275:964–967. [PubMed: 9020076]
29. Fujii H, Hirose T, Oe S, Yasuchika K, Azuma H, Fujikawa T, et al. Contribution of bone marrow cells to liver regeneration after partial hepatectomy in mice. J Hepatol 2002;36:653–659. [PubMed: 11983449]
30. Larrivee B, Niessen K, Pollet I, Corbel SY, Long M, Rossi FM, et al. Minimal contribution of marrow-derived endothelial precursors to tumor vasculature. J Immunol 2005;175:2890–2899. [PubMed: 16116175]
31. Koopmans M, Kremer Hovinga IC, Baelde HJ, de Heer E, Bruijn JA, Bajema IM. Endothelial chimerism in transplantation: looking for needles in a haystack. Transplantation 2006;82:S25–S29. [PubMed: 16829790]
32. Kopp HG, Ramos CA, Rafii S. Contribution of endothelial progenitors and proangiogenic hematopoietic cells to vascularization of tumor and ischemic tissue. Curr Opin Hematol 2006;13:175–181. [PubMed: 16567962]
33. Lalor PF, Lai WK, Curbishley SM, Shetty S, Adams DH. Human hepatic sinusoidal endothelial cells can be distinguished by expression of phenotypic markers related to their specialised functions in vivo. World J Gastroenterol 2006;12:5429–5439. [PubMed: 17006978]
34. Moriga T, Arii S, Takeda Y, Furuyama H, Mizumoto M, Mori A, et al. Protection by vascular endothelial growth factor against sinusoidal endothelial damage and apoptosis induced by cold preservation. Transplantation 2000;69:141–147. [PubMed: 10653393]
35. Li B, Sharpe EE, Maupin AB, Teleron AA, Pyle AL, Carmeliet P, et al. VEGF and PlGF promote adult vasculogenesis by enhancing EPC recruitment and vessel formation at the site of tumor neovascularization. FASEB J 2006;20:1495–1497. [PubMed: 16754748]
36. Gao Z, McAlister VC, Williams GM. Repopulation of liver endothelium by bone-marrow-derived cells. Lancet 2001;357:932–933. [PubMed: 11289353]
37. Ng IO, Chan KL, Shek WH, Lee JM, Fong DY, Lo CM, et al. High frequency of chimerism in transplanted livers. Hepatology 2003;38:989–998. [PubMed: 14512886]
38. Hove WR, van Hoek B, Bajema IM, Ringers J, van Krieken JH, Lagaaij EL. Extensive chimerism in liver transplants: vascular endothelium, bile duct epithelium, and hepatocytes. Liver Transpl 2003;9:552–556. [PubMed: 12783394]
39. Pons JA, Yelamos J, Ramirez P, Oliver-Bonet M, Sanchez A, Rodriguez-Gago M, et al. Endothelial cell chimerism does not influence allograft tolerance in liver transplant patients after withdrawal of immunosuppression. Transplantation 2003;75:1045–1047. [PubMed: 12698096]

Abbreviations

BM
bone marrow

BN
Brown Norway

CIT
cold ischemic time

EGFP
enhanced green fluorescent protein

FACS

NIH-PA Author Manuscript

NIH-PA Author Manuscript

NIH-PA Author Manuscript

fluorescence-activated cell sorting

LEW
Lewis

LSEC
liver sinusoidal endothelial cell

MHC
major histo-compatibility complex

NPC
nonparenchymal cell

OLTx
orthotopic liver transplantation

PBS
phosphate-buffered saline

PI
propidium iodide

SEM
scanning electron microscopy

TEM
transmission electron microscopy

VEGF
vascular endothelial growth factor

VEGF-R2
vascular endothelial growth factor receptor-2

I/R
ischemia/reperfusion

WT
wild-type

NIH-PA Author Manuscript
NIH-PA Author Manuscript
NIH-PA Author Manuscript

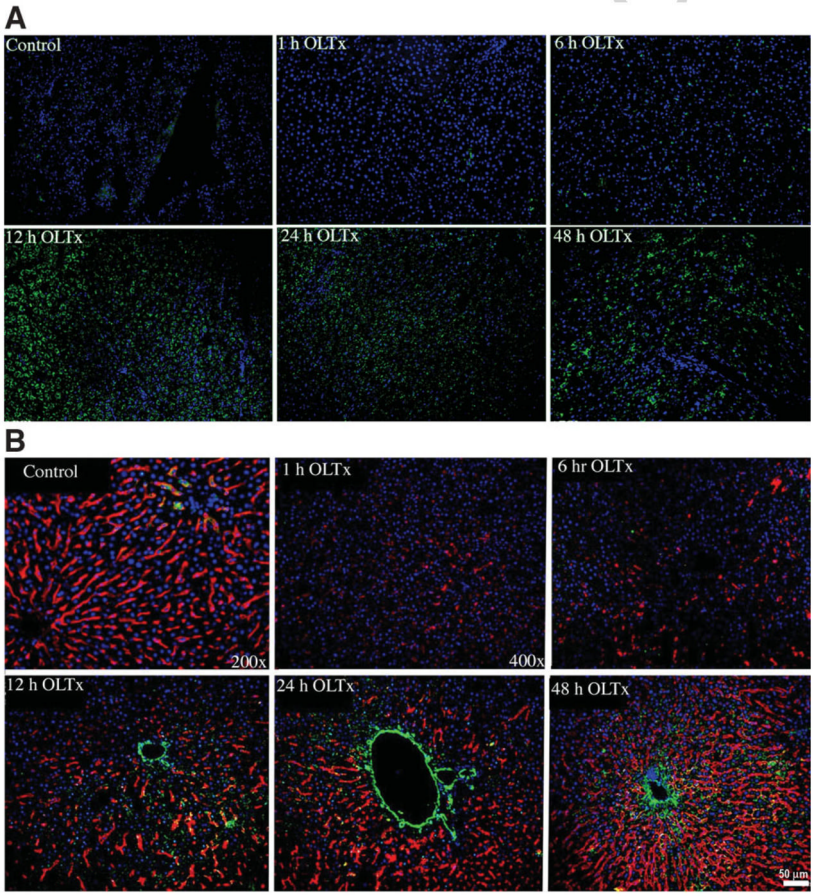

Fig. 1.

VEGF and VEGF-R2 expression in 18-hour CIT-OLTx livers. (A) Time course of VEGF expression (green) in control livers and 1–48 hours after reper-fusion. Low level VEGF signal appears as early as 6 hours post-OLTx, with signal increasing at 12 hours and remaining elevated until 48 hours posttransplantation. (B) Double staining for the LSEC-specific marker SE-1 (red) and VEGF-R2 (green) during the same time period described in panel A. The SE-1 signal is greatly reduced at 1 hour posttransplantation, with graded recovery observed up to 48 hours posttransplantation. A VEGF-R2 signal was observed predominantly in the large vessel endothelium, with scattered positivity within the SE-1 population. VEGF-R2 up-regulation closely parallels the timing of VEGF expression. Nuclei stained with Hoechst (blue). Data are representative of 2 separate experiments.

NIH-PA Author Manuscript

NIH-PA Author Manuscript

NIH-PA Author Manuscript

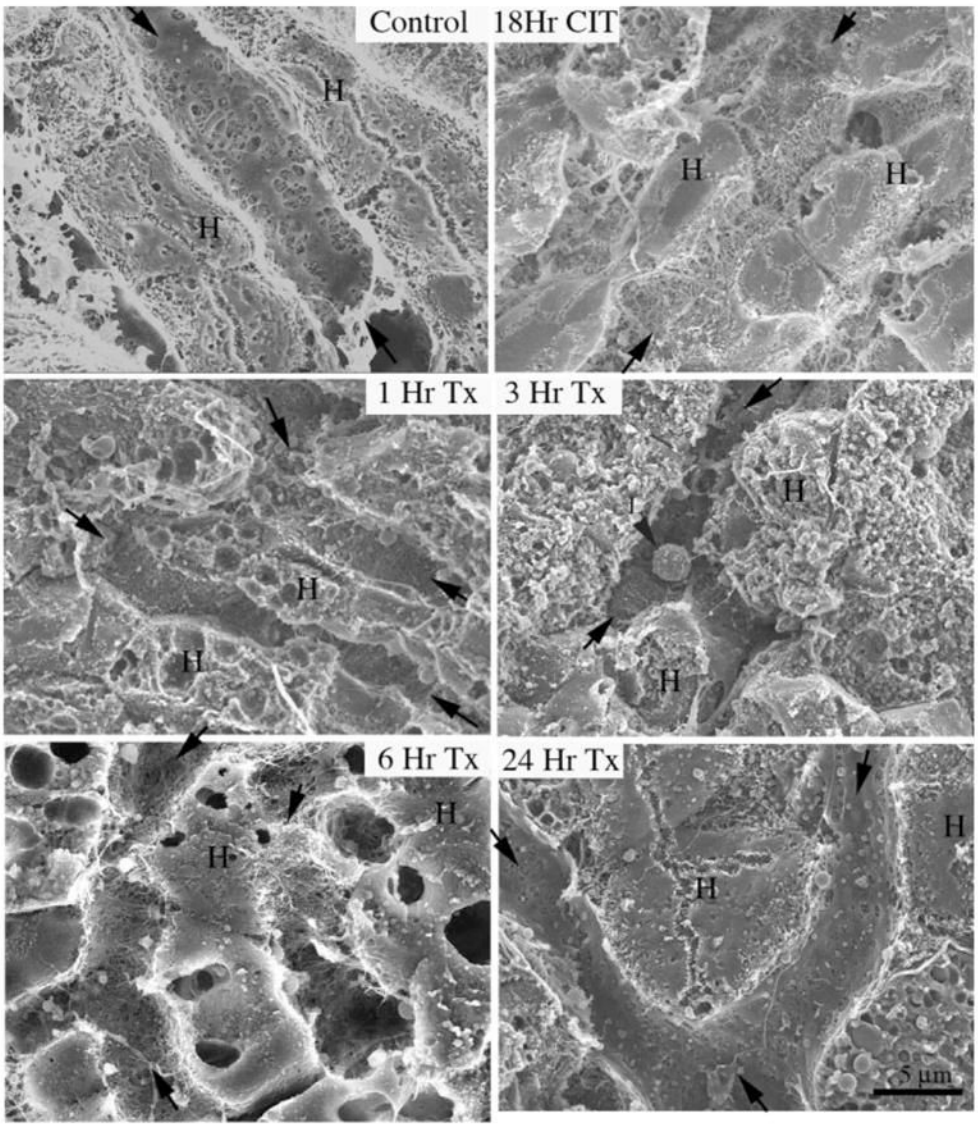

Fig. 2.

SEM evaluation of 18-hour CIT-OLTx livers. Control livers show typical ultrastructural shape, with fenestrated LSECs (arrows) situated between the plates of hepatocytes (H). Eighteen hours after cold ischemic storage before transplantation, sinusoids show partial denudation of LSECs (arrows), while hepatocytes appear normal with recognizable bile canaliculi. One hour after OLTx, LSECs are nearly completely absent in the sinusoids (arrows). Rounded-up remnants of the LSECs are observed clinging to the sinusoid surfaces. Hepatocytes within plates lose their typical ultrastructure with loss of canalicular structure. At 3–6 hours post-OLTx, sinusoids are regaining some LSEC covering. Leukocytes are often observed adhering to the sinusoid surfaces (arrowhead, L). By 6 hours, hepatocytes regain a plate-like shape, and canaliculi are returning. Several areas are regaining LSECs. By 24 hours, most of the sinusoid is recovered by LSECs, although fenestration porosity appears to be reduced. Hepatocytes have also regained their typical shape. Data are representative of 2 separate experiments.

NIH-PA Author Manuscript
NIH-PA Author Manuscript
NIH-PA Author Manuscript

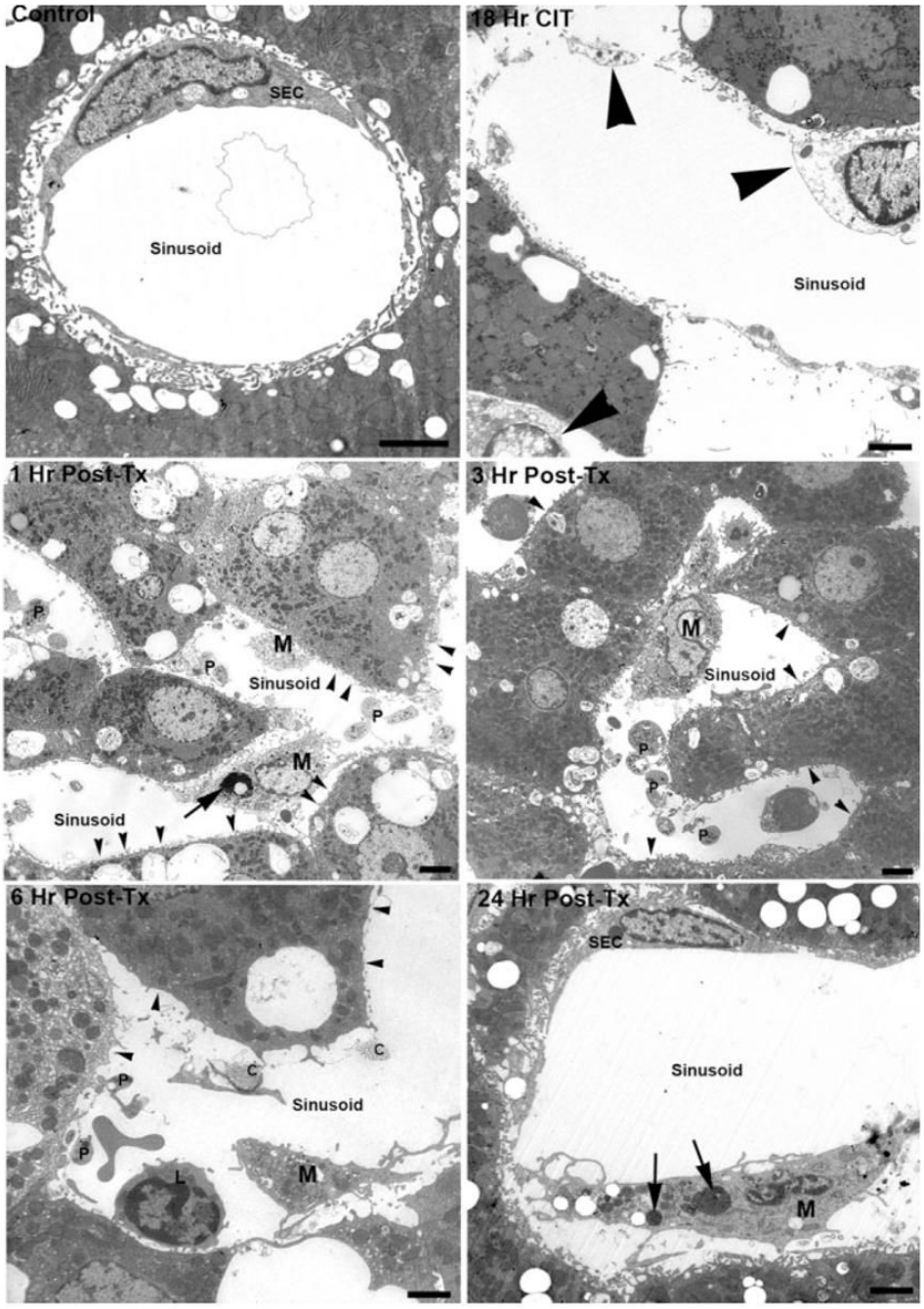

Fig. 3.

TEM evaluation of 18-hour CIT-OLTx livers. Control LSECs display typical fenestrated shape and close association with the hepatocyte microvilli and the space of Disse. After 18-hour CIT, many LSECs are necrotic (arrowheads) and microvilli within the space of Disse are greatly reduced; however, hepatocytes appear to be normal. At 1–6 hours post-OLTx, the entire sinusoid surface is essentially devoid of intact, recognizable LSECs (arrowheads). Hepatocyte microvilli are essentially absent and platelet deposition is apparent (P), as are macrophages (M) with cellular debris inclusions (arrow) and leukocyte adherence (L). Collagen bundles (C) within the space of Disse remain in many areas. By 24 hours post-OLTx, LSECs have largely recovered, as has the ultrastructure within the space of Disse. Macrophages at this time show

large numbers of cellular inclusions packed with cellular debris (arrows). Bars = 2 μm. Data are representitive of 2 separate experiments.

NIH-PA Author Manuscript
NIH-PA Author Manuscript
NIH-PA Author Manuscript

NIH-PA Author Manuscript

NIH-PA Author Manuscript

NIH-PA Author Manuscript

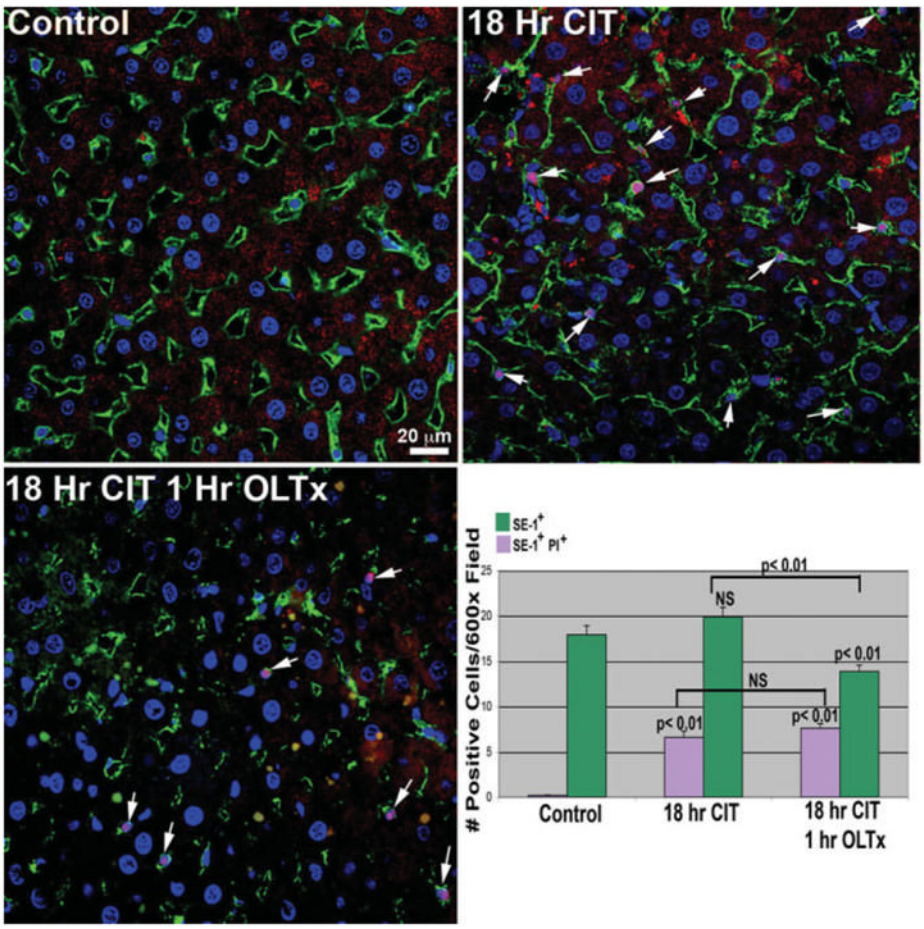

Fig. 4.

LSEC death in 18-hour CIT-stored and 1-hour post-OLTx livers. Livers were processed as described in Materials and Methods, and PI uptake by dead LSECs was evaluated by colocalizing PI nuclear signal (red, arrows) with SE-1^+ cells in the sinusoid (green plasma membrane labeling). No PI labeling is observed in control livers. However, large increases in the pink-stained (red PI stain merged with blue nuclear Hoechst stain) LSECs is observed in both 18-hour CIT livers as well as 1-hour post-OLTx livers. Total LSEC (SE-1^+) and PI^+ LSEC numbers are indicated in the lower right-hand panel. As observed in our initial experiments (Fig. 1), numbers of SE-1^+ cells are significantly decreased 1 hour post-OLTx. There is an increase in the percentage of SE-1^+ cells also positive for PI uptake. Quantitation is the average of 3 animals from each condition; 12 separate 600× images from each animal were analyzed.

NIH-PA Author Manuscript
NIH-PA Author Manuscript
NIH-PA Author Manuscript

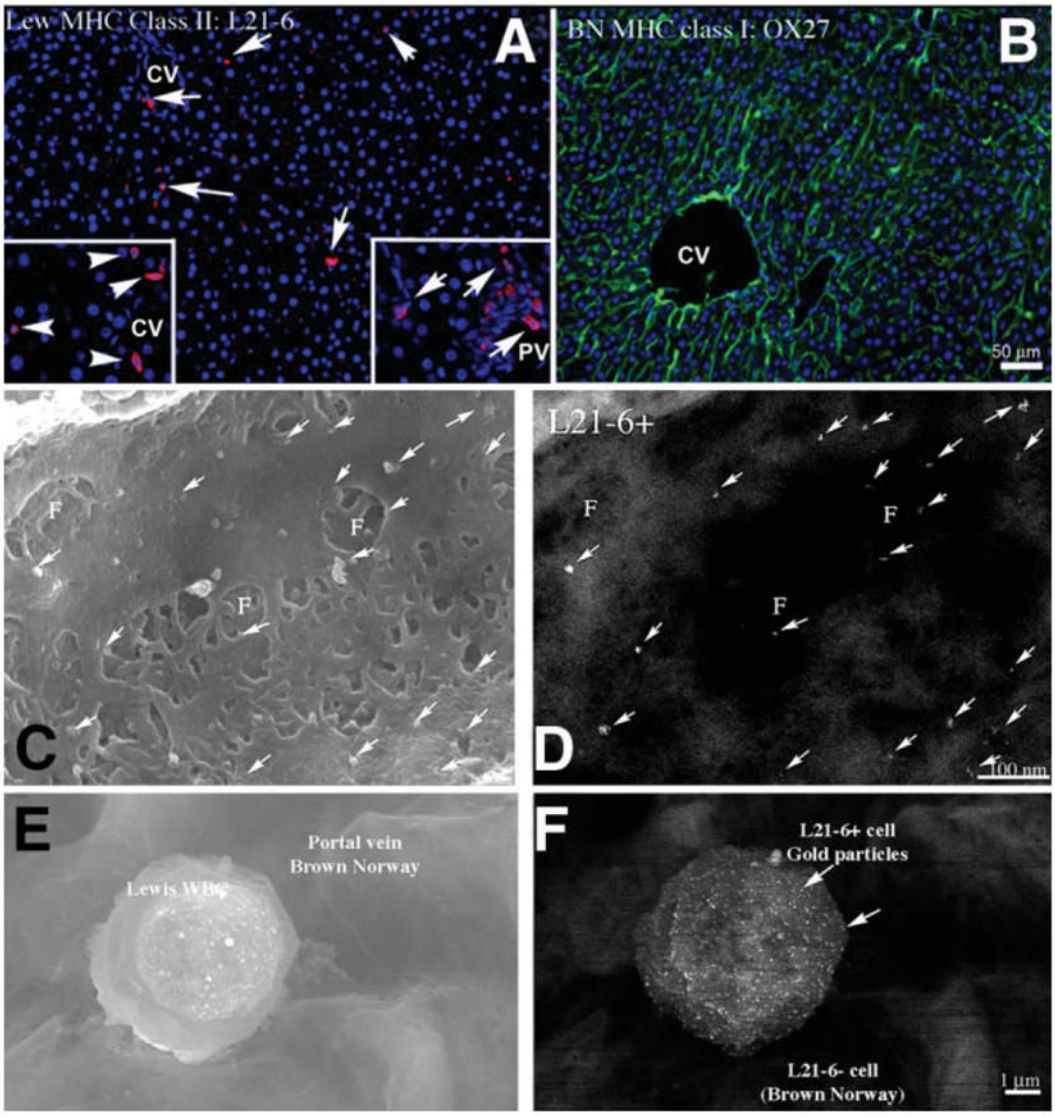

Fig. 5.

Evaluation of recipient LEW cells in BN liver. (A) LEW-specific MHC class II antibody (L21-6) identified LEW cells in the BN donor liver 3 days post-OLTx. Few cells are observed in the sinusoids of the liver (red, arrows), and these cells do not show the flattened shape typical of LSECs. Higher concentrations of L21-6^{+} cells are found in perivascular areas surrounding the central vein (CV, left insert, arrowheads) and in the portal triad (PV, right insert, arrows) but are not integrated into the large vessel intima. (B) Control. BN MHC class I staining of most cell membranes in the transplanted BN rat liver is shown (green). High-resolution immuno-SEM evaluation of an engrafted LSEC of recipient origin was then undertaken. (C) Secondary electron image and (D) parallel backscattered electron image identify the recipient-specific surface marker L21-6 (arrows, 15-nm gold particles) on the surface of a fenestrated LSEC in the BN donor liver sinusoid. Gold particles are on the LSEC, not under the fenestrations. This positive result was seen in 1 out of several hundred cells examined using this technique, indicating it is an uncommon event. (E, F) Secondary electron image and parallel backscattered electron image, respectively, of the typical shape of an L21-6 positive cell in the liver vasculature. This cell is most likely a leukocyte.

NIH-PA Author Manuscript

NIH-PA Author Manuscript

NIH-PA Author Manuscript

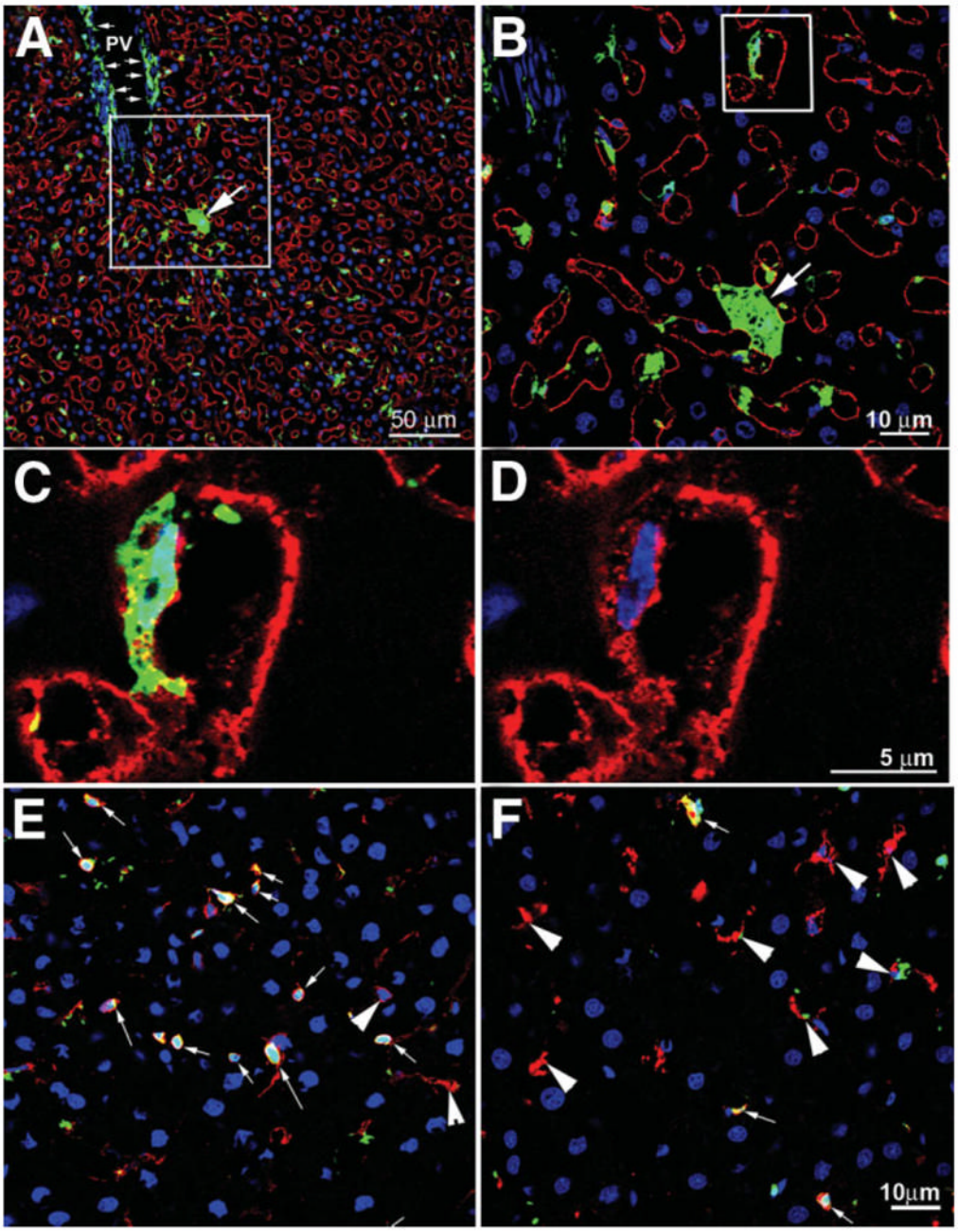

Fig. 6.

EGFP$^+$ BM-derived recipient cells integrating into WT donor livers. (A) Liver harvested from a WT liver transplanted into an EGFP$^+$ recipient 36 days after 18-hour CIT and OLTx. Liver was stained for nucleus (blue) and SE-1 (red). Many EGFP$^+$ cells are scattered throughout the liver, including an EGFP$^+$ hepatocyte (arrow) as well as many perivascular cells surrounding the portal vein (PV, small arrows) and intrasinusoidal cells. (B) The box from panel A is magnified to show the EGFP$^+$ hepatocyte (arrow) as well as an EGFP$^+$ LSEC (box). (C) The box from panel B is magnified to show SE-1$^+$ plasma membrane staining (red) and the EGFP$^+$ and flattened nucleus (blue) of a BM-derived LSEC. (D) Same area as panel C, with the EGFP signal removed to show contiguous SE-1 plasma membrane labeling surrounding a flattened nucleus (blue). (E) Midlobular area colocalizing CD45$^+$ (red) and EGFP$^+$ cells

(arrows). Most EGFP$^+$ cells are leukocytes. A few CD45$^+$ cells are not EGFP$^+$ (arrowheads). (F) Midlobular area colocalizing ED1$^+$ cells (CD68, macrophages, Kupffer cells; red) with EGFP$^+$ cells. Very few ED1$^+$ cells are also EGFP$^+$ (arrows), but most are EGFP$^+$ (arrowheads). These data correlate well with the FACS data from isolated sinusoidal cells presented in Table 3.

NIH-PA Author Manuscript
NIH-PA Author Manuscript
NIH-PA Author Manuscript

NIH-PA Author Manuscript

NIH-PA Author Manuscript

NIH-PA Author Manuscript

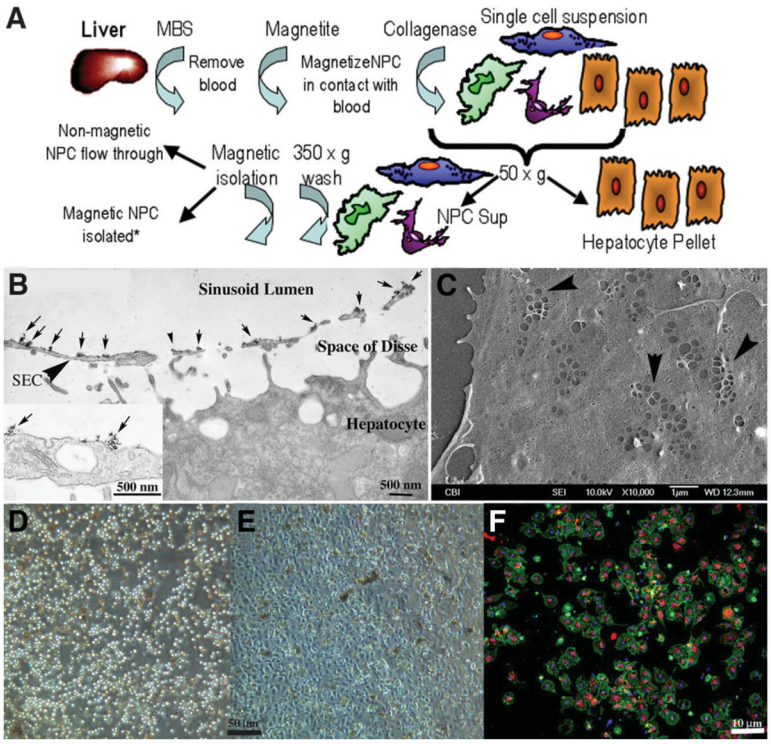

Fig. 7.

(A) Schematic flow diagram outlining isolation of liver sinusoidal NPCs following absorption of cationic magnetite to sinusoidal NPC surfaces. Magnetite perfused through the cleared liver remains adsorbed to NPC membrane surfaces following collagenase perfusion, allowing for specific isolation by MACs columns. *Other liver cells such as hepatocytes, Kupffer cells, and stellate cells can also be isolated and cultured via negative or positive selection (Kupffer cell panning) from the original cell suspension. (B) Transmission electron micrograph of liver fixed immediately after perfusion with cationic colloidal magnetite. Arrows indicate particles of cationic magnetite adsorbed to apical sinusoidal endothelial cell membrane surfaces (arrowhead, SEC). Magnetite particles do not cross through the fenestrated endothelium and do not adsorb to proteins within the space of Disse or the basolateral membrane of the hepatocyte. Inset shows high magnification of magnetite particle clusters on the luminal endothelial cell surface. (C) Scanning electron micrograph of LSECs 24 hours after plating onto collagen-adsorbed coverslip. SECs retain their fenestrations in characteristic sieve plate arrangements (arrowheads). (D) Phase micrograph of original LSEC isolate obtained from the MACs column and plated onto collagen-adsorbed coverslips showing homogeneous cell size. (E) The same isolate 24 hours after plating showing the characteristic cobblestone appearance of endothelium. (F) Uptake of Di-I-acetylated LDL (red) and coincident staining of rat LSEC-specific marker SE-1 (green) in magnetite-isolated LSECs in 24-hour cultures (blue staining indicates Hoechst's dye-stained nuclei).

NIH-PA Author Manuscript

NIH-PA Author Manuscript

NIH-PA Author Manuscript

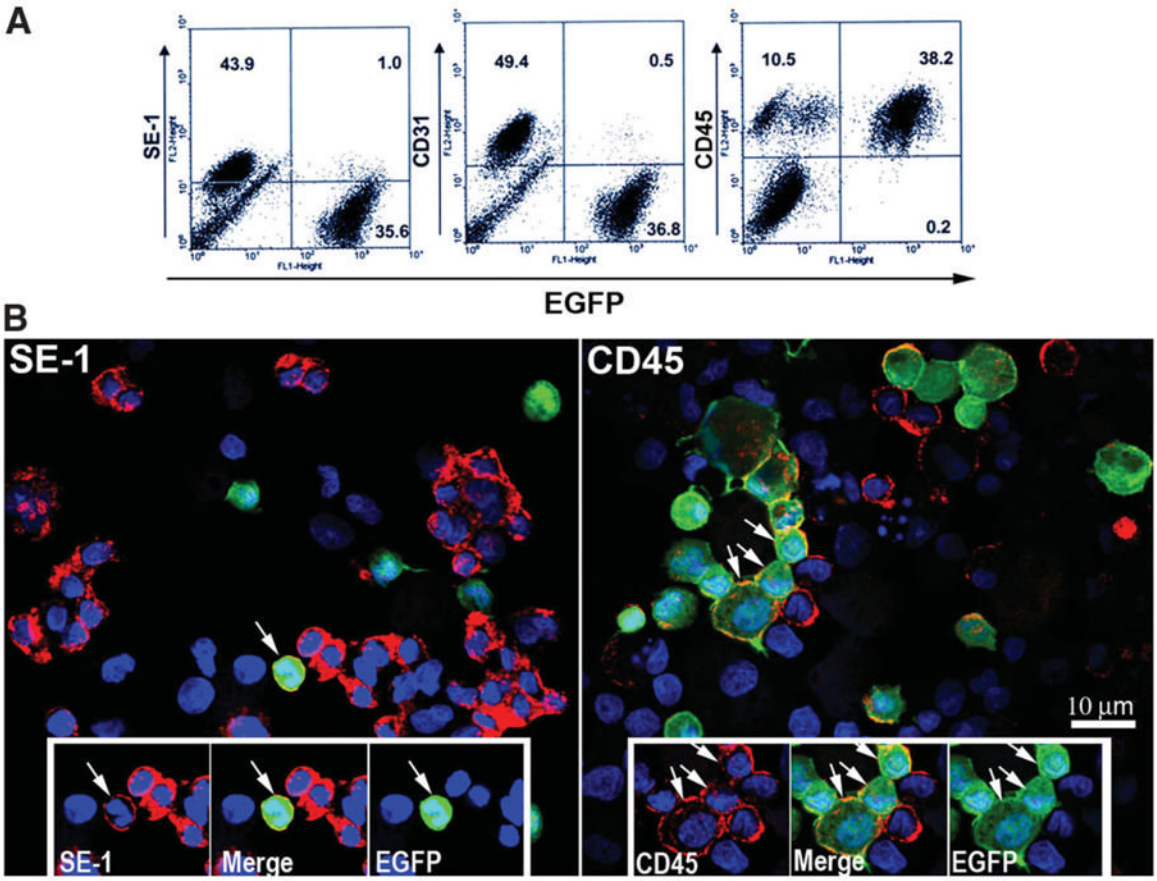

Fig. 8.

Isolation and characterization of origin of sinusoidal cells from an 18-hour CIT WT liver transplanted into an EGFP$^+$ recipient. (A) Cells from a 3-day WT to EGFP$^+$ recipient, 18-hour CIT, post-OLTX liver isolated by cationic magnetite were subjected to FACS analysis for surface markers SE-1 (LSECs), CD31 (large vessel endothelial cells and LSECs), and CD45 (leukocytes). In this particular animal, 1% of the total SE-1$^+$ cells were EGFP$^+$, 0.5% of the CD31$^+$ cells were EGFP$^+$, and 38.2% of the total CD45$^+$ cells were EGFP$^+$, confirming the general trend in the tissue shown in Fig. 6. (B) Cells subjected to FACS analysis were cytospun onto slides, counterstained with Hoechst nuclear stain, and evaluated using confocal fluorescence microscopy. As observed in the FACS and in tissue sections shown in Fig. 7, very few cells colocalize with both SE-1 and EGFP signal (arrow, left panel). Alternatively, many cells were both CD45$^+$ and EGFP$^+$ (arrows, right panel). Insets highlight positive and negative EGFP$^+$ cells for each signal combination.

NIH-PA Author Manuscript

NIH-PA Author Manuscript

NIH-PA Author Manuscript

Table 1

Antibodies and Counterstains Used in This Study

Cells	Epitope	1°Antibody, Clone, Source, Dilution	2°Antibody, Source, Dilution
Rat LSECs	Sinusoidal endothelial cell surface	IF and FACS: mouse anti-rat SE-1 (Dr. Katsuhiko Enomoto, Akita University, Akita, Japan; references [24,25]) 1:100	IF: goat anti-mouse Cy3 (Jackson ImmunoLabs) 1:1000 or goat anti-mouse Alexa 488 (Invitrogen) 1:500 FACS: goat anti-mouse immunoglobulin G phycoerythrin (Invitrogen) 1:100
Large vessel endothelial cells and LSECs, surface	Platelet-endothelial cell adhesion molecule	IF: Mouse anti-rat CD31 (Serotec) 1:100 FACS: Mouse anti-rat CD31 (Chemicon) 1:100	IF: goat anti-mouse Cy3 (Jackson ImmunoLabs) 1:1000 FACS: goat anti-mouse immunoglobulin G phycoerythrin (Invitrogen) 1:100
All leukocytes	Common leukocyte antigen	IF: mouse anti-rat CD45, OX1 (Serotec) 1:100 FACS: mouse anti-rat CD45 conjugated to phycoerythrin, (BD PharMingen) 1:100	IF: goat anti-mouse Cy3 (Jackson ImmunoLabs) 1:1000
Macrophages	Macrophage surface antigen	IF: mouse anti-rat ED2 (CD163) (Serotec) 1:100 FACS: ED2 (CD163)-phycoerythrin (Serotec) 1:10	IF: goat anti-mouse Cy3 (Jackson ImmunoLabs) 1:1000
Macrophages/monocytes	Macrophage marker	IF: mouse anti-rat ED1 (CD68) (Serotec) 1:100	IF: goat anti-mouse Cy3 (Jackson ImmunoLabs, West Grove, PA) 1:1000
LEW cells	Lewis MHC class II	IF and ImmunoGold: mouse anti-Lewis rat MHC class II (L21-6) (Dr. Yuichi Iwaki, University of Pittsburgh, Pittsburgh, PA; reference [27])	IF: goat anti-mouse Cy3 (Jackson ImmunoLabs) 1:1000 ImmunoGold: goat anti-mouse15-nm gold conjugate (Amersham) 1:25
BN cells	MHC class I	IF: mouse anti-BN MHC class I (OX27) (Serotec) 1:400	IF: goat anti-mouse Alexa 488 (Invitrogen) 1:500
VEGF	VEGF	IF: mouse anti-VEGF (Santa Cruz Biotechnology) 1:100	IF: goat anti-mouse Alexa 488 (Invitrogen) 1:500
Endothelial cells	VEGF-R2	IF: rabbit anti-FLK-1 (Santa Cruz Biotechnology) 1:100	IF: goat anti-rabbit Alexa 488 (Invitrogen) 1:500
Endothelial cells	Endothelial cell scavenger receptor	IF: Di-I-acetylated LDL (BTI) 1:250 in culture medium for 4 hours before fixation	This is a vital dye that is endocytosed via the scavenger receptor and therefore is taken up only by live endothelial and macrophages in vitro
Apoptosis marker Counterstain	Annexin V Nucleus	FACS: annexin V-FITC (BD PharMingen) Hoechst 33258: bis-benzimidizole (Sigma) 10 mg/mL PI (Sigma) 0.19 mg/mL	

Manufacturer locations are as follows: Amersham, Piscataway, NJ; BD PharMingen, San Diego, CA; BTI, Stoughton, MA; Chemicon, Temecula, CA; Invitrogen, Carlsbad, CA; Jackson ImmunoLabs, West Grove, PA; Santa Cruz Biotechnology, Santa Cruz, CA; Serotec, Raleigh, NC; Sigma, St. Louis, MO.

Abbreviation: IF, immunofluorescence; FACS, fluorescence-activated cell sorting.

NIH-PA Author Manuscript

NIH-PA Author Manuscript

NIH-PA Author Manuscript

Table 2

Flow Cytometric Analysis of Cationic Colloidal Magnetite-Isolated Sinusoidal Cells Obtained from WT 18-Hour CIT Liver Transplanted into EGFP Recipients

Cell Type	Cell Marker	Percentage of Total Cells Isolated from Sinusoid*	Percentage of $EGFP^+$ Cells†
LSECs	SE-1	42.0 ± 5.0	4.1 ± 2.1
Large vessel endothelial cells/ LSECs	CD31	43.8 ± 7.0	0.4 ± 0.3
Leukocytes	CD45	54.6 ± 7.5	41.2 ± 2.8
Macrophages	ED2 (CD163)	9.30 ± 8.5	4.1 ± 3.6

Sinusoidal cells were isolated 3–7 days after WT liver (18-hour CIT) OLTx into $EGFP^+$ recipients using the cationic magnetite isolation protocol. Cells were then analyzed for specific cell markers* using FACS and for dual positive cell marker/EGFP signal.

† Results are given as the mean ± standard deviation (n = 3).

NIH-PA Author Manuscript
NIH-PA Author Manuscript
NIH-PA Author Manuscript

Table 3

Characterization of Cells Recovered from CIT Liver Exudates

CIT	n	Total Cells (× 10^5/g Liver)	Total Cells (× 10^6/Liver)	SE-1^+ (%)	CD45^+ (%)	SE-1^+/Annexin V^+ (%)
0 hours	2	0.4–3.3	0.96–2.30	41.0–45.5	54.4–58.9	5.7–9.4
18 hours	3	0.3–3.8	0.56–3.96	30.2–54.9	45.2–69.8	4.1–13.1
48 hours	2	0.5–1.9	0.57–14.27	51.4–68.8	31.2–48.6	13.2–14.5

Cells were collected from liver University of Wisconsin storage solution following 0, 18, and 48 hours of CIT and analyzed using FACS for SE-1, CD45, and SE-1^+/annexin V^+ signals. Both LSECs (SE-1^+) and leukocytes (CD45^+) were washed out of the liver after CIT. A small percentage of LSECs were apoptotic as indicated by annexin V staining. Liver graft weights from rats were routinely between 9 and 11 g.

NIH-PA Author Manuscript
NIH-PA Author Manuscript
NIH-PA Author Manuscript

Table 4

Studies Evaluating BM Derivation of Liver Endothelium After Transplantation

Study	Species	Percentage of BM-Derived LSECs	Techniques Used	Microscopy	LSEC Marker	BM Marker
Gao et al.[36]	Human, mouse	Identified, not quantified	X-Y mismatched sex, IHC	Light	Factor VIII	Y,X chromosome
Ng et al.[37]	Human	<1%	X-Y mismatched sex, IHC	Epifluorescence	CD31	Y,X chromosome
Hove et al.[38]	Human	Identified, not quantified	X-Y mismatched sex, recipient HLA, IHC	Light, IHC	Factor VIII	Y,X chromosome
Pons et al.[39]	Human	51 ± 8.28	X-Y mismatched sex, FISH	Epifluorescence	vWF	Y,X chromosome
Present study	Rat	2%–5%	WT graft to EGFP recipient, mismatched recipient MHC	Confocal immunofluorescence, immuno-SEM, flow cytometry	SE-1 fenestrations	Recipient MHC class, EGFP

Abbreviation: IHC, immunohistochemistry.